Global assessment of the carbon–water tradeoff of dry cooling for thermal power generation

Yue Qin [1,2,3] ✉, Yaoping Wang [4], Shiyu Li [2], Hang Deng[3,5], Niko Wanders [6], Joyce Bosmans[7], Liangdian Huang[2], Chaopeng Hong [8,9] ✉, Edward Byers[10], Daniel Gingerich [11,12,13], Jeffrey M. Bielicki [11,13,14] & Gang He [15,16]

Water scarcity and climate change are dual challenges that could potentially threaten energy security. Yet, integrated water–carbon management frameworks coupling diverse water- and carbon-mitigation technologies at high spatial heterogeneity are largely underdeveloped. Here we build a global unit-level framework to investigate the CO_2 emission and energy penalty due to the deployment of dry cooling—a critical water mitigation strategy—together with alternative water sourcing and carbon capture and storage under climate scenarios. We find that CO_2 emission and energy penalty for dry cooling units are location and climate specific (for example, 1–15% of power output), often demonstrating notably faster efficiency losses than rising temperature, especially under the high climate change scenario. Despite energy and CO_2 penalties associated with alternative water treatment and carbon capture and storage utilization, increasing wastewater and brine water accessibility provide potential alternatives to dry cooling for water scarcity alleviation, whereas CO_2 storage can help to mitigate dry cooling-associated CO_2 emission tradeoffs when alternative water supply is insufficient. By demonstrating an integrative planning framework, our study highlights the importance of integrated power sector planning under interconnected dual water–carbon challenges.

Thermal electric power generation uses substantial amounts of freshwater primarily for cooling, amounting to approximately 40–50% of total water withdrawal in the United States and 40% in Europe[1–3]. Meanwhile, power generation accounts for approximately 36% of energy-related carbon dioxide (CO_2) emissions across advanced economies in 2019, placing the power sector among the world's largest CO_2 emitters[4]. Consequently, the power sector has a high dependence on freshwater resources and demonstrates intrinsic water–carbon interconnections, which thereby have critical implications on reliable electricity output and energy security, particularly under climate change[5,6].

With increasing recognition of the inherent water–carbon interconnections in electricity generation, growing studies have been calling for integrated water and energy systems planning[3,7]. Previous work mostly focuses on the water–energy nexus via evaluating the climate impacts on usable electricity generation capacity and associated power sector vulnerability due to water quantity and water temperature changes[8–13]. Recent efforts unravelling the power sector water–carbon linkages often centre on those more popular fuel switch strategies (for example, switching from coal to natural gas[14,15] and to low/no-water consuming renewables[16,17]). In comparison, the underlying water–carbon interactions for critical water mitigation and retrofitting technologies in power sector water management have been relatively under evaluated, particularly for the most progressive water-mitigating yet energy-consuming dry cooling techniques, which

---

A full list of affiliations appears at the end of the paper. ✉e-mail: qinyue@pku.edu.cn; hcp12@tsinghua.org.cn

are often analysed within limited geographic locations[6,10,18], at aggregated resolutions[18], or treated with relatively simplified assumptions[19]. Meanwhile, an increasing amount of studies are developing global consistent high-resolution unconventional water resource datasets[20–22], which advance the evaluation of the potential role of alternative water sources (for example, wastewater and brine water) in alleviating water stress[6,23,24], although, so far, they often do not focus on the power sector or are constrained in limited geographic regions[6].

Facing increasing water scarcity concerns, dry cooling has been and may continually be promoted as an emerging freshwater mitigation technique in some major economies in the next few decades along with renewable energy transition[5,18]. In spite of its water saving characteristics, dry cooling is disadvantaged by higher costs and larger land footprints. Most notably, it suffers from reduced efficiencies due to two key factors: the use of fans to increase airflow required for steam condensation results in an additional parasitic load, thus reducing the useful electrical output of the plant; and higher temperature results in a higher 'backpressure' (for example, a negative pressure that has to be overcome for the steam flow to continue), which reduces the temperature gradient across the steam turbine and thus also reduces the electrical output. Combined, these factors increase fuel consumption and CO_2 emissions per unit of electricity produced[2,3,18]. Given the intrinsic water–carbon interlinkages, dry cooling could provide one of the best examples to illustrate the role of integrated power planning, especially in the context of alternative water sourcing and carbon mitigation technologies in resolving the dual challenges of water scarcity and climate change. However, the geospatial variations, temporal trends, and potential technology substitutes for dry cooling-associated water–carbon interactions have not been systematically evaluated at the global scale, thereby inevitably hindering an integrated and proactive power sector planning.

In this Article, we design a global unit-level integrated framework to systematically investigate dry cooling-associated water–carbon interactions by coupling alternative water-sourcing and carbon-mitigating technologies. Integrating location-specific generation units (for example, fuel type and installed capacity) and local meteorology (for example, air temperature and relative humidity), together with water properties (for example, water temperature and runoff), we first characterize the geospatial patterns of dry cooling-associated water–carbon interconnections. We then identify global hotspots that could be particularly vulnerable for dry cooling deployment due to increasing efficiency losses under climate warming scenarios. Integrating information on alternative water sourcing and CO_2 mitigation techniques, we further explore utilizing alternative sources of cooling water and CO_2 storage capacity to better tackle the dual challenges of water scarcity and climate change via establishing an integrated cooling technology–alternative water sourcing–CO_2 storage framework.

Age-based water–carbon interactions for dry cooling units

Figure 1 demonstrates the age structure of global fossil (for example, coal, natural gas and oil) and non-fossil (for example, biomass, solar and nuclear) dry cooling units in 2015 broken down by major countries/regions. We observe three dominant global features. First, fossil fleets dominate dry cooling generation units. Among ~177 GW global major dry cooling units evaluated here in 2015, coal accounted for ~86% (152 GW) of total operational capacity, followed by natural gas (12%, 21 GW) and oil (1.2%, 2.1 GW) fleets (Supplementary Fig. 1). Second, dry cooling units are younger than generation units equipped with other cooling technologies, indicating a much more recent development and deployment. In 2015, approximately 51% (91 GW) and 82% (146 GW) of dry cooling generation capacity were less than 5 and 10 years old, respectively. In comparison, roughly 25% (44%) and 10% (16%) of recirculating and once-through-freshwater generation units are less than 5 (10) years old[25], respectively. Once-through has historically been the

dominant cooling technology due to its relatively simple design and low costs, and the fact that earlier power plants are often built close to abundant water resources[3,26]. However, with increasing concerns on local water scarcity, thermal pollution, ecological disruption and therein growing regulatory pressure[27], recirculating and dry cooling are now favoured both in the design of new plants and major retrofits[25]. Until more recently, dry cooling generation units have historically only been used in a few countries. In particular, China alone contributes ~73% of global total dry cooling capacity, almost all of which are coal units (Supplementary Fig. 1). South Africa, the United States, Iran and India also have notable dry cooling capacity; although other than in South Africa and India, most are non-coal units (for example, a large chunk of natural gas dry cooling fleets are in the United States). Consequently, dry cooling-associated water–carbon tradeoffs are most evident in China, South Africa and India, where dry cooling units primarily burn high carbon-emitting coal.

Dry cooling-induced freshwater mitigation is achieved at the expense of increased CO_2 emissions. As illustrated in Fig. 1a,d and Supplementary Fig. 2, among dry cooling fossil fleets, increased CO_2 emissions and avoided water withdrawal across age groups are roughly in proportion to their respective generation capacity, although less so for non-fossil fleets. Globally, dry cooling techniques applied to major fuel types avoid approximately 75 and 0.4 billion cubic metres (bcm) of water withdrawal and water consumption, respectively, equalling to roughly complete water withdrawal and 84% of water consumption mitigation in comparison to once-through cooling. These water savings are achieved at the expense of approximately 39 million tonnes (Mt) of increased CO_2 emissions, that is around 5% extra emissions when compared with once-through cooling. In comparison, switching from recirculating to dry cooling can save 1.3 (95%) and 1.9 bcm (93%) of water withdrawal and water consumption, respectively, at the expense of approximately 34 Mt (6%) increases in CO_2 emissions. This demonstrates apparent dry cooling-induced water–carbon tradeoffs, particularly for notable water withdrawal mitigation.

Geospatial variations in water–carbon interactions

The spatial pattern of dry cooling deployment has large implications on local water scarcity, location-specific efficiency loss, CO_2 emissions, and hence the water–carbon interactions, in comparison to counterfactual cases of once-through (Fig. 2) and recirculating (Supplementary Fig. 3) cooling utilization. Across the globe, unit-level avoided water withdrawal ranges from ~0.4 to 800 million m^3 per year in comparison to once-through cooling and ~0.01 to 15 million m^3 per year in comparison with recirculating cooling, respectively. The largest unit-level avoided water withdrawal is primarily centred in northern China, western United States, and southern Africa. Cross-unit variations in avoided water withdrawal for the same counterfactual cooling techniques are mainly due to differences in unit-level electricity generation and in water withdrawal coefficients owing to different fuel types and location-specific meteorology. Retrofitting from once-through to dry cooling, on average saves roughly 50 times more water withdrawal, than switching from recirculating to dry cooling (Fig. 2a and Supplementary Fig. 3a), primarily due to orders of magnitude larger water withdrawal coefficients of once-through fleets than other cooling techniques[19]. The spatial pattern of avoided water consumption is largely resembling that of avoided water withdrawal, yet water consumption savings are larger when retrofitting from recirculating cooling to dry cooling than switching from once-through to dry cooling, but their differences are much smaller (~2.5 times) than water withdrawal (Supplementary Fig. 4).

Increases in efficiency loss and CO_2 emissions demonstrate notably different spatial patterns to the patterns of avoided water withdrawal. Overall, dry cooling efficiency losses are roughly 1.4–15% and 1.3–13% (as a percentage of electricity output) higher than once-through and recirculating cooling, with the hotspots of high-efficiency-loss
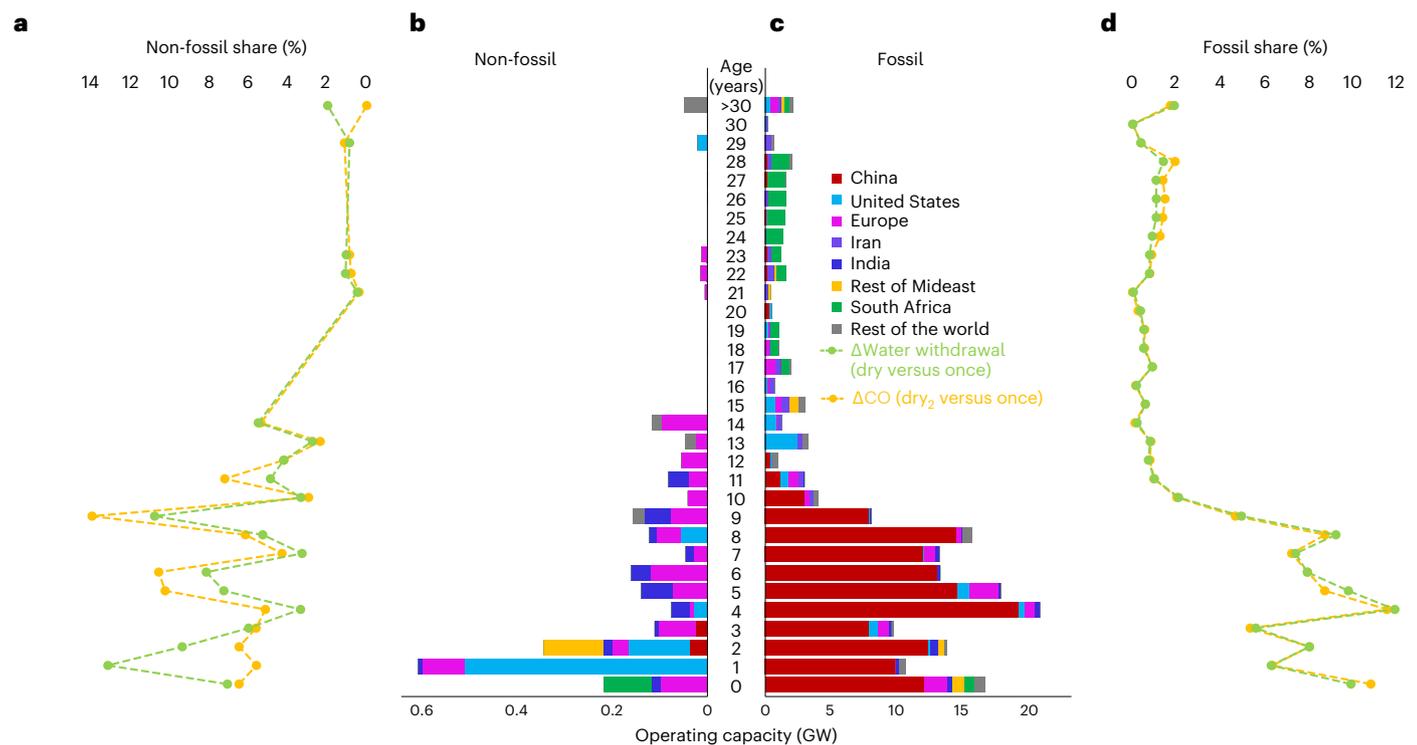
Fig. 1 | Age structure of global dry cooling generation capacity and associated water–carbon interactions. a,d, Curves indicate the estimated percentage of avoided water withdrawal (ΔWater withdrawal) and increased CO_2 emissions (ΔCO$_2$) from each age cohort to the sum of all ages' non-fossil (**a**) and fossil (**d**) dry cooling units in comparison with counterfactual cases of once-through freshwater cooling (dry versus once). **b,c,** The operating capacity of non-fossil (**b**) and fossil (**c**) units where the youngest fleets are at the bottom.

The dominance of young fleets indicates an apparent more recent dry cooling technology deployment. Here, generation units that began operating in 2015 are defined as 0 years old. Age-specific avoided water withdrawal and consumption, together with increased CO_2 emissions for dry cooling units in comparison with counterfactual cases of once-through and recirculating cooling are shown in Supplementary Fig. 2.

concentrating around India, Southeast Asia and southern parts of Africa. Units with high levels of increased CO_2 emissions are primarily centred around India and northern China (that is, 0–550 kilo tonnes in comparison with once-through cooling and 0–510 kilo tonnes to recirculating cooling), where dry cooling units mostly use coal as input fuel and have relatively high efficiency loss and/or large generation capacity. Geospatial patterns of dry cooling-associated efficiency loss increases do not resemble that of CO_2 emission increases as generation units' installed capacity and fuel-specific carbon emission factors also vary by region. Despite notable dry cooling-induced water savings, the associated CO_2 emissions can be substantial. In particular, due to high ambient temperature exposure and dominating coal fleets in India, it is among the global hotspots of high carbon penalties (that is, increased CO_2 emissions) with per unit avoided water withdrawal (Supplementary Fig. 5).

### Tackling dry cooling fleets with high-efficiency loss

We observe substantial variations in dry cooling units' associated efficiency losses across fuel types, geographic regions and seasons predominantly driven by exposure to high ambient temperature (Fig. 3 and Supplementary Fig. 6), which could provide potential targeted mitigation opportunities via utilizing alternative water sources or carbon mitigation technologies.

Primarily driven by ambient temperature (Supplementary Fig. 6a), oil fleets have the largest fraction of units exposed to relatively high efficiency loss (that is, efficiency loss as a fraction of expected power generation ≥7.5%), followed by biomass and coal units. High-efficiency loss biomass fleets contribute roughly 30% of total generation capacity and avoided water withdrawal, and almost 45–50% of increased CO_2 emissions. To a lesser degree, a similar pattern is observed for coal fleets. Due

to the dominating coal share within dry cooling fleets (~86%), it makes up the largest total amount of high-efficiency loss dry cooling units (~24 GW out of 29 GW). In comparison, natural gas fleets have a much larger share of low-efficiency loss units (that is, efficiency loss as a fraction of expected power generation <2.5%), with roughly 8% of fleets exposed to high-efficiency loss, which contributes ~10% of avoided water withdrawal and ~15% of increased CO_2 emissions. A large share of high-efficiency loss oil, biomass and coal dry cooling fleets raises critical concerns regarding water–carbon tradeoffs. Although CO_2 emissions from biomass combustion are considered close to carbon neutral, high-efficiency loss biomass and fossil fleets potentially provide targeted carbon mitigation opportunities via carbon capture and storage (CCS)[28,29].

Likewise, across geographical regions, Africa has the highest proportion of units exposed to high efficiency loss due to a large portion of units exposed to high temperature (Supplementary Fig. 6b), with roughly 80% (~9.7 GW) of such operating capacity. In comparison, a much smaller share of dry cooling generation capacity in Asia (~12%), North America (~4%) and Europe (~1%) are high-efficiency loss units. Nevertheless, with the largest quantity of dry cooling generation capacity (~140 GW), Asia alone (~17 GW) contributes ~55% of global total high-efficiency loss units, highlighting regions exposed to the largest resulting energy and carbon penalties.

Additionally, as over 90% of dry cooling fleets are concentrated in the northern hemisphere, we observe a strikingly larger fraction of high-efficiency loss dry cooling fleets in northern hemisphere summer than in the three other seasons due to higher summer temperature (Supplementary Fig. 6c). For example, in June–July–August, high-efficiency loss fleets make up ~85% of seasonal total installed dry cooling capacity, compared with merely 8–13% of fleets exposed to high efficiency loss in other three seasons.
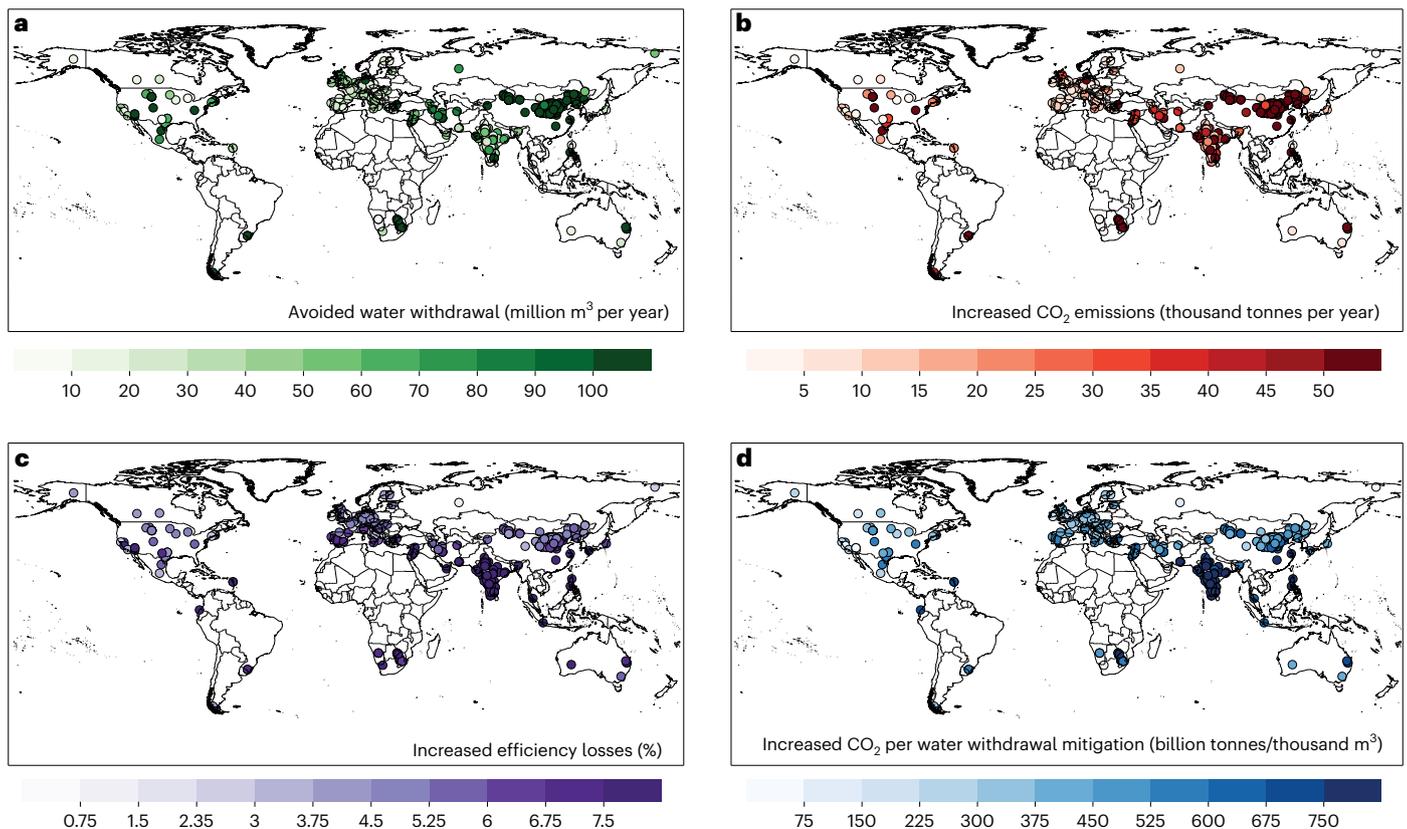
Fig. 2 | Spatial pattern of global dry cooling generation units associated water–carbon interactions. a–d, Geospatial distribution of unit-level avoided water withdrawal (**a**), increases in CO_2 emissions (**b**), increases in energy efficiency loss (**c**) and increased CO_2 emissions per avoided water withdrawal (**d**) for dry cooling units compared with once-through freshwater cooling.

The geospatial heterogeneities in water withdrawal mitigation and carbon penalty is apparent. Map comparisons with recirculating cooling are shown in Supplementary Fig. 3. Global basemaps are based on Natural Earth[53] and plotted with Python 3.9.13.

## Increasing efficiency loss under a warming climate

Increasing ambient temperature under a warming climate generally leads to higher backpressure and consequently non-linearly increasing higher efficiency loss for dry cooling units, which could thereby threaten a reliable electricity output (Supplementary Table 1 and Extended Data Fig. 1). On global average, other than RCP2.6, we observe a consistent increase in both ambient temperature and efficiency loss over the years, with the most striking increases observed under RCP8.5. Global weighted average efficiency loss of dry cooling units increases from ~6.4% in 2020–2029 to 6.7% and 7.1% in 2050–2059 and to 7.4% and 8.4% in 2090–2099 under RCP6.0 and RCP8.5, respectively, indicating a proportional electricity generation loss from dry cooling fleets. Notably, dry cooling fleets' efficiency loss generally demonstrates faster increases than ambient temperature, particularly under RCP8.5 (Fig. 4, Extended Data Fig. 1 and Supplementary Fig. 7). Figure 4d–f illustrates the spatial pattern of the relative scaling factors of efficiency loss to ambient temperature under each RCP scenario, which further highlights a faster-than-temperature increase in efficiency losses under a warming climate, particularly under RCP8.5. Similar trends are also observed for once-through and recirculating cooling units, with the most prominent efficiency losses under the high climate scenario (Supplementary Figs. 8–11).

Integrated power sector planning under climate change

Under expected intensifying droughts[30,31], increasing water demand[32] and stricter regulations[18], dry cooling techniques may play a more important role before renewables could largely substitute fossil

fleets. Hence here we explore a hypothetical case that, among global thermal units exposed to high water scarcity (that is, water scarcity index (WSI) >0.4 (refs. 32,33)) that are not currently equipped with dry cooling techniques (that is, once-through and recirculating cooling, Supplementary Fig. 12), what would their efficiency loss be if they were retrofitted to dry cooling to avoid further water scarcity. Figure 5a shows units-specific efficiency loss if dry cooling were employed, showing generation fleets with high-efficiency loss and sizeable capacity are primarily concentrated in India, eastern China, western Europe, Southeastern Asia and southern United States, signalling the necessity to integrate alternative technologies into power sector planning.

Thereby, we further explore the potential role of alternative water sourcing (for example, wastewater and brine water with commercial prospects (C-brine); Methods) and CO_2 storage in resolving dry cooling-associated water–carbon tradeoffs if generation units would suffer from relatively high-efficiency loss when switching to dry cooling (blue points in Fig. 5a). Figure 5b–e shows the ratio of location-specific total cooling water withdrawal to alternative water availability. Increasing the reusable proportion—share of wastewater reused (WWr) to total produced wastewater (WWp)—plays a most important role in providing sufficient alternative water, while increasing the collection distance for wastewater and brine water can also substantially increase alternative water availability. If all WWp could be reused with a collection distance of 25 km, the proportion of thermal generation capacity whose cooling water demand could be fully satisfied (that is, satisfiable portion) via wastewater and brine water would increase from 25% (WWr+C-brine) to 85% (WWp+C-brine). In comparison, increasing alternative water
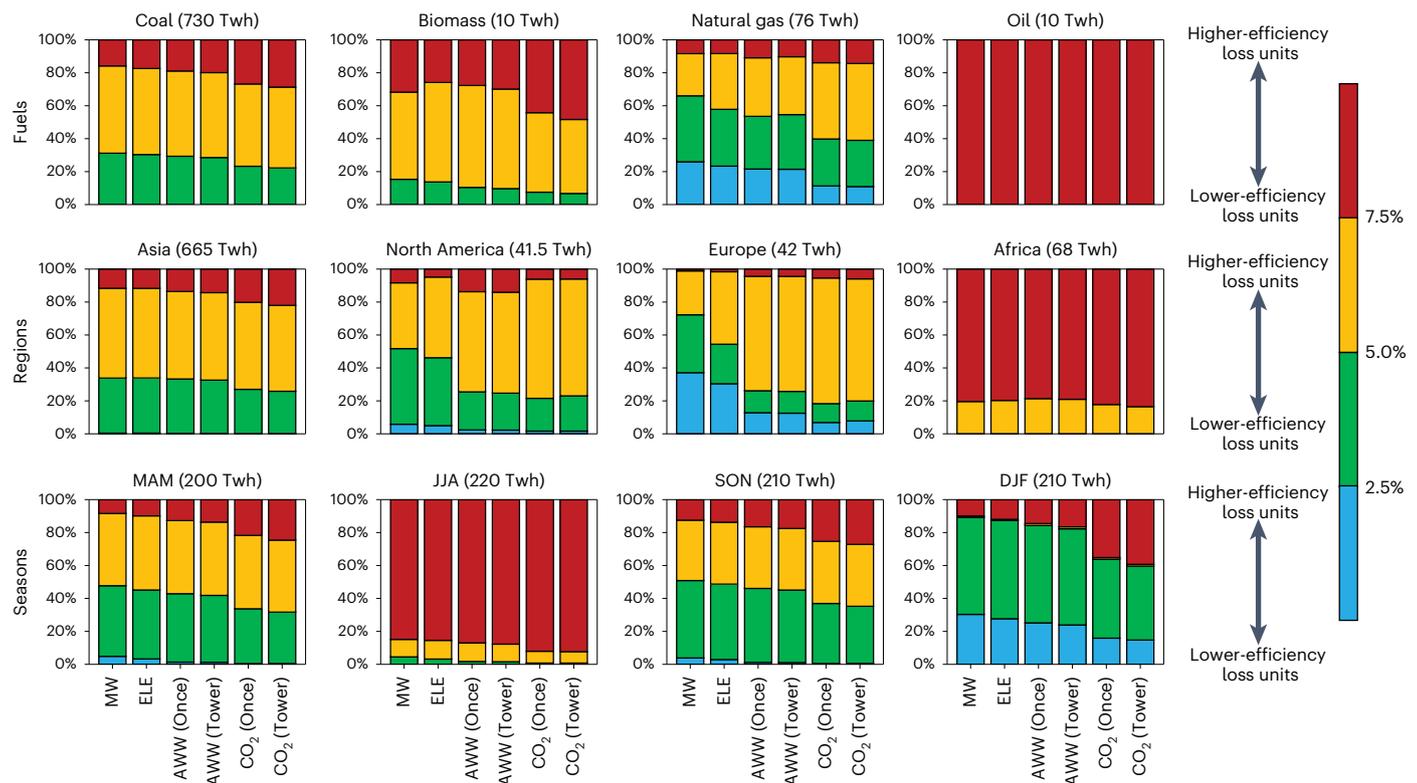
Fig. 3 | Share of generation capacity and water–carbon impacts by efficiency loss. In each panel, bars from left to right show the fraction of installed capacity (MW), electricity generation (ELE), avoided water withdrawal relating to once-through (AWW (Once)) and recirculating (AWW (Tower)) cooling, and increased CO_2 emissions relating to once-through (CO_2 (Once)) and recirculating (CO_2 (Tower)) cooling. Six vertical bars in each panel are composed of units with four levels of dry cooling units' efficiency loss. Panels are broken down by major fuel types, regions and seasons. Biomass CO_2 emissions are shown to indicate potential carbon capture opportunities, although they are considered close to carbon neutral. Numbers on top of each panel represent total electricity generation for specific fuel types, regions, and seasons.

(WWr+C-brine) collection distance from 10 to 50 km, this share could increase from 15% to 42%.

As currently identified commercially ready CO_2 storage and the associated brine water (C-brine) is relatively small, the satisfiable portion is predominately provided by wastewater (Supplementary Fig. 13a,b). Therefore, the brine water extraction rates from commercially ready carbon storage candidate sites have negligible impacts on the satisfiable portion. Nevertheless, global total geologic CO_2 storage capacity and the corresponding brine water availability identified by the United States Geological Survey (USGS) are notably larger than those identified with relatively high commercial readiness[34] (Supplementary Figs. 14 and 15). Thus, if global total geologic CO_2 storage capacity can be developed, the associated extractable brine water together with reusable wastewater (WWr+USGS-brine, Fig. 5e) can meet roughly 63% of thermal water demand under 25 km collection distance, and could further increase to 73% when expanding the collection distance to 50 km (Supplementary Fig. 16a). As brine water availability associated with candidate USGS carbon storage sites (USGS-brine) is much larger, it can surpass WWr in meeting thermal generation water demand, although still smaller than WWp (Supplementary Fig. 13c and 16b). For generation units whose nearby alternative water is insufficient in meeting their water withdrawal (for example, magenta points in Fig. 5e), we thereby still have to rely on dry cooling for water scarcity alleviation, and hence further turn to carbon storage to resolve dry cooling-induced CO_2 emission increases. Roughly 19.5 GW out of 141 GW (magenta points in Fig. 5e), that is, ~14% of thermal generation capacity, have access to nearby USGS geological CO_2 storage (25 km accessibility distance). Therefore, other strategies (for example, switching to fuel types requiring no/low water uses, wind turbine and solar photovoltaic

(PV); inter-basin water transfer) may be needed for those remaining units without close access to CO_2 storage, particularly in India, eastern China and Thailand (Fig. 5f).

Therefore, challenges exist in largely relying on currently reusable wastewater and brine water (for example, particularly C-brine) to substitute dry cooling in alleviating water scarcity or relying on potential carbon storage to address dry cooling-induced CO_2 penalties, especially considering there will be increasing energy consumption and/or water uses accompanying alternative water treatment and CCS (Supplementary Notes, Supplementary Figs. 17 and 18, and Supplementary Tables 2 and 3)[18]. That said, thermal units are mostly dominated by net water savings and CO_2 emission reductions (Supplementary Figs. 17–19). Therefore, increasing reusable wastewater and more progressive brine water extraction (for example, USGS-brine) to substitute for dry cooling, or alternatively, dry cooling coupled with CO_2 storage, can still potentially provide important opportunities to partly resolve power sector-associated water–carbon tradeoffs.

Discussion

Cooling water availability directly affects thermoelectric power generation capacity and electricity system reliability[8,9]. Climate-induced changing water availability together with intensifying cross-sector water-use competition[9,10,32,35] are expected to pose increasing threats to the global power system that has a strong dependence on freshwater resources[3,6] and contributes substantial CO_2 emissions, which can further aggravate climate change[36]. Therefore, an integrated power sector design to address the underlying water–carbon nexus is essential. In particular, dry cooling serves as a great candidate to illustrate integrated power planning via coupling water use reduction (that is,
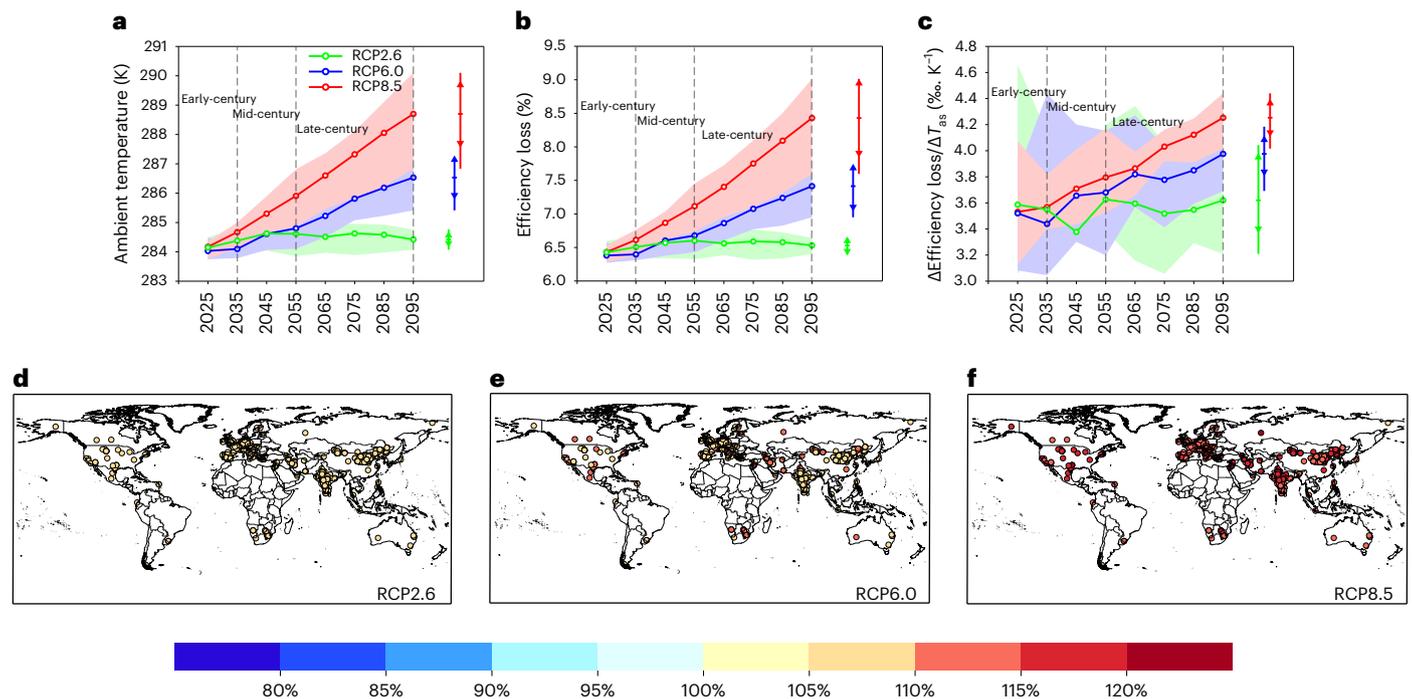
Fig. 4 | Increasing dry cooling units' efficiency loss under a warming climate. **a**–**c**, The temporal evolvement of ambient temperature (T_{as}) (**a**), efficiency loss (**b**), and their relative increasing rates (**c**) in comparison to history (1996–2005) (ΔEfficiency loss/ΔT_{as}) under different climate warming scenarios (early century: 2020–2039, mid-century: 2040–2059, and late century: 2060–2099) for existing global dry cooling generation units weighted by generation capacity. As we use 10 year average GCM output, 2025 indicates the average value of the period of 2020–2029 and so on. In **a**–**c**, coloured shadings indicate multi-model ranges for each RCP scenario; coloured vertical lines represent the corresponding value ranges in 2090–2099, with the whole range, the triangles and the short horizontal line representing the minimum–maximum, 25th and 75th and mean values, respectively. **d**–**f**, Spatial pattern of efficiency loss scaling factor in 2050–2059 relative to the beginning of the simulating period (2020–2029) to the T_{as} scaling factor (((Efficiency loss$_{2050-2059}$/Efficiency loss$_{2020-2029}$) / ($T_{as2050-2059}$/$T_{as2020-2029}$)) for each warming scenario (RCP2.6 (**d**), RCP6.0 (**e**), RCP8.5 (**f**)). Global basemaps are based on Natural Earth53 and plotted with Python 3.9.13. Unit-level efficiency loss responses to ambient temperature and scaling factors for 2090–2099 are shown in Extended Data Fig. 1 and Supplementary Fig. 7.

dry cooling), water supply expansion (that is, alternative water sourcing) and CO$_2$ mitigation (that is, carbon storage) technologies due to its intrinsic water–carbon tradeoffs.

Despite dry cooling consistently reducing water use at the expense of increased energy consumption and/or CO$_2$ emissions, it demonstrates notable heterogenies regarding the magnitude of dry cooling-associated energy penalties and efficiency losses across fuel types, geographic regions, and four seasons. Such variations are primarily driven by dry cooling fleets' exposure to ambient temperature, with higher temperature exposure inducing higher backpressure, which thereby generally requires extra energy to overcome the backpressure and consequently causes higher energy penalty and lower overall energy efficiency (Supplementary Fig. 6). Such characteristics could thereby pose critical challenges to dry cooling units for freshwater mitigation and energy security. Dry cooling is mostly needed in drought and arid regions that are exposed to high water scarcity; with an expected intensifying water scarcity under a warming climate, there may be an increasing reliance on dry cooling techniques. However, owing to mostly faster increasing rates in efficiency loss than in ambient temperature for dry cooling fleets, dry cooling-associated water–carbon tradeoffs could be further intensified under climate change. Global weighted average efficiency loss, and hence associated electricity losses of dry cooling units, can reach 6.7% and 7.1% in 2050–2059 and 7.4% and 8.4% in 2090–2099 under RCP6.0 and RCP8.5, respectively.

This is particularly concerning under the warmest scenario, especially in regions such as India, where large amounts of generation fleets are already exposed to high water scarcity and where both thermal generation capacity are expected to further increase, yet the associated efficiency losses and corresponding electricity generation loss of local dry cooling fleets can exceed 15% in the middle of the century under a warming climate. Consequently, a warming climate could induce higher dependence on dry cooling, yet simultaneously make it less energy efficient and pose potential threats to local energy supply, especially when dry cooling is largely employed and under notably high temperature. In that vein, additional water- and carbon-mitigation strategies are also needed to better resolve the dual challenges of water scarcity and climate change.

Unconventional water supply (for example, wastewater and brine water) can potentially compensate for freshwater inadequacy to alleviate water scarcity. With a collection distance of 25 km, WWr, total WWp, commercially ready brine water (C-brine) and total geological brine water (USGS-brine) can individually meet 24.3%, 85.1%, 0.9% and 56.3% of thermal water demand, or 39.4%, 96.6%, 3.2% and 61.1% under 50 km, respectively, demonstrating both total produced wastewater and USGS-brine water can largely substitute dry cooling in tackling water scarcity, highlighting the importance of increasing the reusable proportion of wastewater, expanding alternative water collection distance and progressive brine water extraction. When nearby alternative water is insufficient to substitute dry cooling in mitigating water scarcity, USGS carbon storage can help to tackle dry cooling-induced CO$_2$ emission penalties. In spite of extra energy and/or water demand for alternative water treatment and CCS employment, alternative water sources and carbon storage can generally provide important opportunities to resolve the water–carbon tradeoffs in the power sector (Supplementary Figs. 17–19). Such trends are generally consistent under a changing climate (Supplementary Figs. 20 and 21).

Limitations and uncertainties apply to this study. First, we focus on unit-level cooling technology deployment together with grid-level
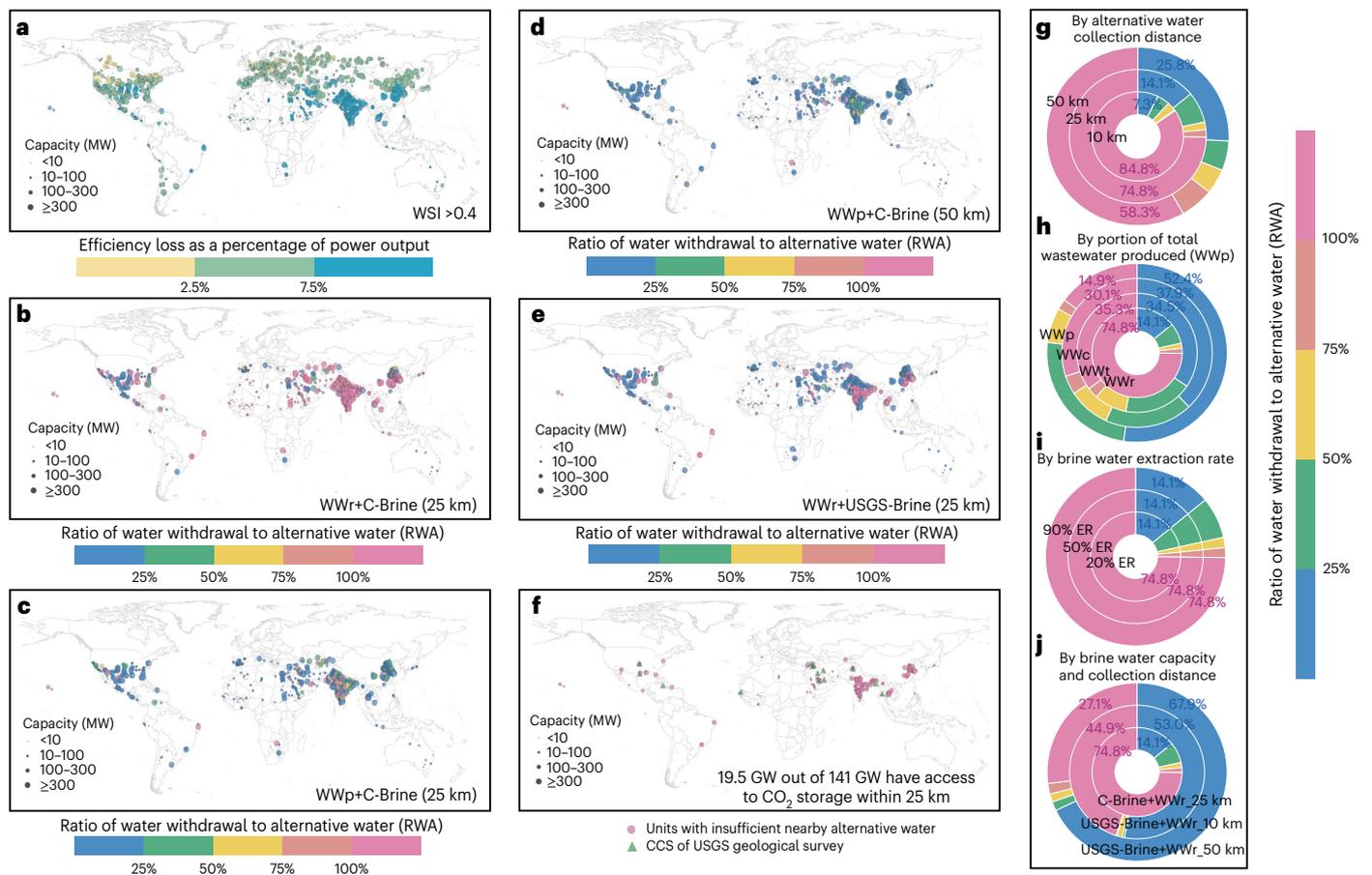
Fig. 5 | Historical integrated dry cooling with alternative water sourcing and carbon mitigation. a, Unit-level efficiency loss for thermal generation units if equipped with dry cooling exposed to historical high water scarcity (WSI >0.4) (1996–2005). **b–e**, Ratio of grid-level total cooling water withdrawal to alternative water sources (wastewater and brine water) (RWA) for magenta high-efficiency loss units if equipped with dry cooling in **a**. Alternative water sources refer to: the sum of intentional reusable wastewater and potentially commercial-ready brine water with a collection distance of 25 km (WWr+C-Brine) (**b**), the sum of total produced wastewater and C-Brine (WWp+C-Brine) with a collection distance of 25 km (**c**) and 50 km (**d**), and the sum of intentional reusable wastewater and brine water based on the USGS geological survey (WWr+USGS-Brine) with a collection distance of 25 km (**e**). Brine water extraction rates in are all 50% (**b–e**).

f, Accessibility to nearby USGS carbon storage for generation units lacking sufficient alternative water (magenta dots in **e**). Global basemaps are based on Natural Earth53 and plotted with Python v. 3.9.13. **g–j**, Pie charts show the relative share of generation capacity falling into different levels of RWA, varying by alternative water (WWr+C-Brine) collection distance (10 to 50 km) (**g**), the portion (WWr, WWt, WWc) of total wastewater produced (WWp) (**h**), brine water extraction rates (ER) (20% to 90%) (**i**), and brine water capacity (C-Brine to USGS-Brine) and collection distance (10 to 50 km) (**j**). Numbers in **g–j** indicate the proportion of operating generation capacity belonging to the lowest (≤25%, blue) and highest (>100%, magenta) RWA level. RWA ≤100% indicate alternative water is sufficient to substitute dry cooling for freshwater mitigation.

alternative water sourcing and site-specific carbon storage information to establish an integrated power planning framework. Yet, factors such as inter-basin water transfer, groundwater pumping, and virtual water transfer are not considered in our current unit-level framework, as such high-resolution data are still largely lacking across the globe. When future fine-resolution data becomes available, we can incorporate such information into our unit-level framework for improvement. Second, our estimated brine water is conservative as we only consider brine extraction from candidate CO$_2$ storage sites. This is because brine extraction from CO$_2$ storage sites can serve as a pressure management practice to prevent potential hazards such as land subsidence via CO$_2$ injection, and largely reduce brine extraction costs as it may be partially covered by geological carbon storage. Third, our results can potentially be affected by uncertainties in climate internal variability, we thereby rely on multi-model ensemble means in combination with the model spreads to represent the most likely results together with the uncertainty ranges. Supplementary Figs. 22 and 23 show the standard deviation and coefficient of variation on unit-level efficiency losses based on model-specific results, indicating our results are generally

robust across climate models. Fourth, here we only consider dry cooling generation units directly recorded in the world electric power plants database, which may have underestimated total dry cooling capacity. However, the spatial and temporal patterns of dry cooling-associated water–carbon tradeoffs are consistent, and the integrated framework can be extended to other dry cooling units in a relatively straightforward manner.

As our integrated framework also identifies the global hotspots where neither dry cooling nor alternative water sourcing or carbon storage are capable of easily resolving the water-carbon tradeoffs from thermal generation (for example, India and east China in Fig. 5f), our study thereby also indicates where switching to no- or low-water consuming renewables (for example, wind and PV) are most needed from the water scarcity alleviation perspective, indicating potential water-oriented power sector transition pathways along with the worldwide carbon neutrality pursuit. Because of the intrinsic water–carbon interlinkages, it is important to also factor into water concerns in designing worldwide power sector decarbonization pathways, particularly for regions such as India and Africa that may

simultaneously suffer from intensifying water scarcity and increasing energy demand.

By systematically unravelling unit-level water–carbon interlinkages associated with dry cooling in the context of alternative water sourcing and carbon storage, our study provides a global-scale unit-level framework for integrated power sector planning, which is becoming increasingly indispensable under complex challenges facing human populations.

Methods

Unit-level water use and CO_2 emissions

We estimate unit-level water withdrawal, water consumption and CO_2 emissions for global dry cooling generation units operating in 2015, primarily based on the World Electric Power Plants database (2017 version) (https://www.spglobal.com)[37], which provides basic power generation units information, such as fuel types, engine types, installed capacity, cooling technology and administrative-level company information[25]. We then obtain unit-level geo-coordinates and additional information from Qin et al.[25], which primarily extract information from existing power databases (for example, the Carbon Monitoring for Action Database (CARMA) and the Emissions & Generation Resource Integrated Database (eGRID)), the World Cities information and Google application programming interfaces (APIs). We estimate unit-level electricity generation by multiplying each unit's installed capacity and its corresponding capacity factor. We obtain fuel-specific CO_2 emission factors from the Intergovernmental Panel on Climate Change reports (https://www.ipcc-nggip.iges.or.jp/public/2006gl/). Water withdrawal and water consumption coefficients for different generation units are obtained on the basis of earlier studies[19,25,38–41]. For each generation unit, we then estimate its CO_2 emissions, water withdrawal and water consumption based on unit-level electricity generation and corresponding emission factors, water withdrawal and water consumption coefficients. Note we include CO_2 emission estimation from biomass combustion, which are considered close to be carbon neutral, as it can potentially provide carbon mitigation opportunities via CCS.

Unit-level efficiency loss

We estimate unit-level efficiency loss on the basis of the World Electric Power Plants database and hydrological model outputs. We first simulate grid-level water temperature using the PCRaster Global Water Balance model version 2 (PCR-GLOBWB 2), a state-of-the-art grid-level global hydrology and water resources model, at 5 arc-minutes spatial resolution[42,43], which has five major modules: meteorological forcing, land surface, groundwater, surface water routing, and irrigation and water use[42]. Five global climate models (GCM models: GFDL-ESM2M, HadGEM2-ES, IPSL-CM5A-LR, MIROC-ESM-CHEM and NorESM1-M) from the Inter-Sectoral Impact Model Intercomparison Project (ISIMIP) forced by three different representative concentration pathway emissions scenarios (RCP2.6, RCP6.0 and RCP8.5) in the Coupled Model Intercomparison Project Phase 5 are used in this study to provide input meteorological variables (for example, air temperature, air pressure and humidity) at the spatial resolution of 0.5 × 0.5 degrees for PCR-GLOBWB 2 model and our estimation of unit-level efficiency loss. As explained in earlier studies[44,45], PCR-GLOBWB 2 employs an improved water temperature module compared with the previous energy balance model, which leads to better comparison between water temperature simulation and observation due to improved physical realism (for example, additional processes to cover ice breaking up and larger water bodies thermal mixing). Refer to Sutanudjaja et al. for more details on PCR-GLOBWB 2 (ref. 42). For each GCM and RCP scenario combination, we conduct simulations for both the historical (1996–2005) period and the future climate (2020–2099). Ten year monthly mean values (for example, 1996–2005) from each model output under each RCP scenario are used to represent the average historical and future climate conditions.

With the same end-use electricity output, power generation units equipped with dry cooling technology have notable efficiency loss and associated energy and/or carbon penalty (that is, increased energy consumption and CO_2 emissions) due to higher backpressure and lower efficiency of steam turbines, as well as more energy consumption for fans and pump operations[10,46]. We focus on the energy penalty in steam turbines and combined cycle power plants (for example, coal, natural gas, oil, biomass, nuclear and concentrated solar power). Based on grid-level 10 year monthly average meteorological inputs and water temperature outputs of the PCR-GLOBWB 2 model and unit-level technology information (for example, fuel types and installed capacity), we estimate energy penalty for global dry cooling generation units using equations (1)–(5). For each dry cooling generation unit, we also estimate its counterfactual efficiency loss, assuming once-through or recirculating cooling technology were employed instead (equation (6)). We then compare the relative efficiency losses, as well as changes in water withdrawal, water consumption and CO_2 emissions for those dry cooling fleets as in comparison with the hypothetical cases of once-through and recirculating cooling, respectively (Fig. 2 and Supplementary Fig. 3).

Steam turbine efficiency loss as a percentage of designed electricity output ($\Delta\eta$) is a function of turbine pressure (p, inches Hg). Following earlier studies[46], equations (1)–(4) are used to estimate turbine backpressure for fossil steam (including biomass, 67% load), nuclear (100% load), combined cycle (67% load) and other generation units (67% load), respectively. As pointed out in earlier studies, nuclear fleets often used as the baseload mostly operate closer to full capacity (represented by the 100% load curve), yet fossil units often operate closer to the 67% load curve[46]. Backpressure here refers to engine-produced exhaust gas pressure to overcome the exhaust system's hydraulic resistance, so as to allow steam flow to continue. Thereby, increasing backpressure associated with wet and dry cooling towers will lead to reduced turbine efficiencies and consequently power generation penalties. T_{as} and T_{in} represent ambient air temperature (°F) and condenser inlet temperature (°F), respectively[46]. The condenser inlet temperature is estimated as water temperature for once-through cooling generation units, while it is estimated as cooling tower outlet temperature for recirculating cooling generation units[46]. Cooling tower performance is largely determined by the difference between wet bulb temperature and the cooling tower outlet temperature, which is referred to as tower approach[10,46]. In addition to steam turbine efficiency loss, cooling generation units also lose efficiency due to fans and pumping equipment, as summarized below. Therefore, efficiency loss in this study is estimated as a percentage of designed electricity output[46]. We further classify dry cooling units into four classes roughly following the 25th (2.5%), 50th (5%) and 75th (7.5%) percentiles of unit-level efficiency loss.

Based on historical unit-level efficiency losses for dry cooling units, we sum up their generation capacity and electricity generation, as well as dry cooling fleets' avoided water withdrawal and increased CO_2 emissions, in comparison with water-cooling technologies, by major fuel types, regions and seasons (Fig. 3). Such targeted opportunities identify fuel types, geographic regions and seasons when or where efficiency losses are particularly high for dry cooling generation units, which hence require particular attention.

On top of that, we further analyse the changes in unit-level and aggregated efficiency losses for dry cooling fleets under different climate scenarios (Fig. 4 and Extended Data Fig. 1). We categorize the future years into three time periods: early century (2020–2039), mid-century (2040–2059) and late century (2060–2099). While existing dry cooling units are most likely to be retired in early and mid-century, we still provide the efficiency losses for the whole future period up to 2099, as our primary focus is to evaluate the potential efficiency losses evolution for existing or similar dry cooling generation units under different levels of future climate (RCP2.6, RCP6.0 and RCP8.5). In addition, we also evaluate efficiency loss changes for the counterfactual retrofitting

cases of dry cooling units to once-through and recirculating cooling (Supplementary Fig. 8).

1. Turbine efficiency loss (as a percentage of designed power output)

$$\text{Combustible steam}\Delta = 0.0063 \times p^2 - 0.004 \times p - 0.0062 \quad (1)$$

$$\text{Nuclear steam}\Delta\eta = -0.0006 \times p^3 + 0.0099 \\ \times p^2 - 0.0208 \times p + 0.0111 \quad (2)$$

$$\text{Nonnuclear noncombustible steam}\Delta\eta = -0.0013 \times p^3 \\ +0.0169 \times p^2 - 0.0286 \times p + 0.0098 \quad (3)$$

$$\text{Combined cycle}\Delta\eta = -0.0004 \times p^3 + 0.0082 \times p^2 - 0.016 \times p + 0.0033 \quad (4)$$

2. Exhaust backpressure (inches Hg)

$$\text{Dry } p = 1.031 \times \exp(0.019 \times T_{as}) \quad (5)$$

$$\text{Once through/Recirculating } p = 0.4591 \times \exp(0.0213 \times T_{in}) \quad (6)$$

3. Fans and pumping energy use (as a percentage of designed power output)[46]

	Combustible steam	Non-combustible steam	Combined cycle
Dry	2.43%	0.56%	0.81%
Once-through	3.04%	1.18%	0.15%
Recirculating	0.45%	1.48%	0.39%

Alternative water sourcing and carbon mitigation technology
The PCR-GLOBWB 2 model provides runoff and sector-specific water withdrawal, including agricultural (irrigation and livestock), industrial and municipal water withdrawal[42,45,47]. We then estimate grid-level (0.5 × 0.5 degrees) WSI using equation (7) based on available total runoff and water withdrawal data for the historical period (1996–2005) for climate models (that is, GFDL-ESM2M, HadGEM2-ES and IPSL-CM5A-LR) obtained from the ISIMIP online platform (ISIMIP 2b) (https://www.isimip.org). WSI is a widely used index to indicate the relative level of water scarcity. WSI of 0.4 is usually used in prior studies as the threshold to indicate whether or not a region is exposed to high water scarcity[48], with a larger WSI indicating a higher water scarcity. WSI <0.1 indicates low water scarcity, 0.2 > WSI ≥ 0.1 indicates moderate water scarcity, and 0.4 ≥ WSI ≥ 0.2 indicates medium water scarcity. WSI reflects the relative share of water available that is used (for example, withdrawal-to-availability resource ratio). In our study, we primarily focus on high water scarcity (WSI >0.4), with the same threshold (WSI = 0.4) used for different regions and time periods to indicate the spatial and temporal heterogeneities in water scarcity across the world and with changing climate. As not all freshwater can be used by human population (for example, environmental flow needs), WSI >0.4 is widely considered to be a reasonable though not definitive threshold value[48].

$$\text{WSI} = W/Q \quad (7)$$

W refers to PCR-GLOBWB 2 simulated total water withdrawal: adding agricultural, industry and domestic water withdrawal; Q refers to PCR-GLOBWB 2 simulated total runoff.

Increasing concerns on water scarcity are expected to facilitate further deployment of dry cooling techniques in the next decade or so before a dominating penetration of wind and solar PV becomes feasible.

This, however, may lead to notable water–carbon tradeoffs due to much higher efficiency losses for dry cooling fleets, especially for thermal units in hot and arid regions. Therefore, we further integrate alternative water sources (that is, wastewater and brine water) and carbon storage into power sector technology planning, such that to explore opportunities in resolving dry cooling-associated water–carbon tradeoffs.

We first integrate thermal generation units with grid-level global baseline water scarcity map to identify different generation units' exposure to local water scarcity. Globally, we assume dry cooling techniques can potentially be employed across the locations where thermal (that is, here includes fossil and biomass) generation units use freshwater for cooling purposes and are exposed to high water scarcity (WSI >0.4). Supposing dry cooling technique is employed, we then estimate the resulting unit-level efficiency loss and CO_2 emissions for supplying per unit (MWh) additional electricity. We emphasize that here we do not mean to predict future penetration rates of dry cooling techniques. Instead, we try to explore whether existing thermal generation units' locations would be suitable for utilizing dry cooling for alleviating water stress, considering the underlying water–carbon linkages. As PCR-GLOBWB 2 model does not include thermoelectric cooling water withdrawal for power generation, our estimated WSI is conservative.

For generation units suffering from notable efficiency loss if dry cooling were utilized in water scarcity alleviation, we further explore the possibility of using alternative water sources to substitute dry cooling in mitigating freshwater dependence. Due to substantial treatment costs of wastewater and brackish water, we assume once-through cooling will be retrofitted to recirculating cooling when relying on alternative water for water scarcity alleviation. We obtain grid-level wastewater availability from Jones et al.[21], which summarizes domestic and manufacturing total WWp (359.4 bcm per year), collection (WWc, 225.6 bcm per year), treatment (WWt, 188.1 bcm per year) and intentional WWr (40.7 bcm per year) at 5 arc-minutes resolution. Notably, untreated wastewater can also be reused intentionally, while both treated and untreated wastewater can be reused unintentionally, which are not included in WWr[21]. Refer to Jones et al.[21] for more details on global wastewater data. We consider a series of collection distances (for example, 10 km, 25 km and 50 km) to capture the range of wastewater accessibility for generation units requiring alternative water sources. Supplementary Table 2 summarizes extra energy consumption and associated CO_2 emission intensities for wastewater treatment (Supplementary Notes).

Additionally, we obtain CO_2 storage with commercial prospect together with brine water availability based on the CO_2 Storage Resource Catalogue Cycle 2, which assessed over 700 CO_2 Storage Resources sites, including both saline aquifers, as well as oil and gas fields[49]. The CO_2 Storage Resource Catalogue is a second update of the Oil and Gas Climate Initiative funded programme aiming at gaining commercial readiness of geologic CO_2 storage resources across global key markets[49]. Similarly, we assume a collection distance ranging from 10 to 25 and 50 km, with a series of brine extraction ratios of 20% (low), 50% (mid) and 90% (high)[50–52]. Among locations with notable water–carbon tradeoffs, if dry cooling were employed, alternative water sourcing can be utilized to substitute dry cooling if sufficient alternative water (for example, wastewater and/or brine water) are available. We only consider brine extraction from candidate CO_2 storage sites. This is because brine extraction from CO_2 storage is considered a pressure management practice, which will inject CO_2 while extracting brine water, which can therefore prevent potential hazards such as land subsidence due to brine extraction. In addition, because brine extraction is a pressure management practice for CO_2 storage, the cost of brine extraction may be partially covered by geological carbon storage. However, if alternative wastewater and brine water are insufficient, dry cooling technique will then still be needed for freshwater mitigation while emitting additional CO_2 emissions. Hence we further evaluate those units' nearby geologic CO_2 storage capacity to explore site-specific difficulty in tackling dry cooling-associated CO_2 penalty

(for example, increasing CO_2 emissions). In addition to currently identified CO_2 storage capacity with commercial prospects, we also evaluate global geological potential of carbon storage and the associated brine water capacity based on the United States Geological Survey (https://certmapper.cr.usgs.gov/data/apps/world-maps/), which is much larger than those with commercial prospects. Supplementary Tables 2 and 3 summarize extra energy consumption, associated CO_2 emissions and water demand intensities for brine water treatment and for conducting CCS. We further estimate the extra energy (and associated CO_2 emissions) and water for CCS deployment and alternative water (wastewater and brine water) treatment, which may (partly) dampen the role of alternative water and CCS in resolving dry cooling-associated water–carbon tradeoffs (Supplementary Notes).

Reporting summary

Further information on research design is available in the Nature Portfolio Reporting Summary linked to this article.

Data availability

Data used to perform this work can be found in Supplementary Information. Numerical results for Figs. 1–5 and Extended Data Fig. 1 will be provided with this paper as source data, any further data that support the findings of this study are available from the corresponding authors upon request. Source data are provided with this paper.

Code availability

Computer code or algorithm used to generate results that are reported in the paper and central to the main claims are available from the corresponding authors upon request.

References

1. King, C. W., Holman, A. S. & Webber, M. E. Thirst for energy. *Nat. Geosci.* **1**, 283–286 (2008).
2. Webster, M., Donohoo, P. & Palmintier, B. Water–CO_2 trade-offs in electricity generation planning. *Nat. Clim. Change* **3**, 1029–1032 (2013).
3. Sanders, K. T. Critical review: uncharted waters? The future of the electricity–water nexus. *Environ. Sci. Technol.* **49**, 51–66 (2015).
4. Liu, Z. et al. Carbon Monitor, a near-real-time daily dataset of global CO_2 emission from fossil fuel and cement production. *Sci. Data* **7**, 392 (2020).
5. Zhang, C., Zhong, L. & Wang, J. Decoupling between water use and thermoelectric power generation growth in China. *Nat. Energy* **3**, 792–799 (2018).
6. Tidwell, V. C., Macknick, J., Zemlick, K., Sanchez, J. & Woldeyesus, T. Transitioning to zero freshwater withdrawal in the U.S. for thermoelectric generation. *Appl. Energy* **131**, 508–516 (2014).
7. Siddiqi, A., Kajenthira, A. & DíazAnadónb, L. Bridging decision networks for integrated water and energy planning. *Energy Strategy Rev.* **2**, 46–58 (2013).
8. Van Vliet, M. T. H. et al. Vulnerability of US and European electricity supply to climate change. *Nat. Clim. Change* **2**, 676–681 (2012).
9. van Vliet, M. T. H., Wiberg, D., Leduc, S. & Riahi, K. Power-generation system vulnerability and adaptation to changes in climate and water resources. *Nat. Clim. Change* **6**, 375 (2016).
10. Wang, Y. et al. Vulnerability of existing and planned coal-fired power plants in Developing Asia to changes in climate and water resources. *Energy Environ. Sci.* **12**, 3164–3181 (2019).
11. van Vliet, M. T. H., Vogele, S. & Rubbelke, D. Water constraints on European power supply under climate change: impacts on electricity prices. *Environ. Res. Lett.* https://doi.org/10.1088/1748-9326/8/3/035010 (2013).
12. van Vliet, M. T. H. et al. Multi-model assessment of global hydropower and cooling water discharge potential under climate change. *Glob. Environ. Change* **40**, 156–170 (2016).
13. Behrens, P., van Vliet, M. T. H., Nanninga, T., Walsh, B. & Rodrigues, J. F. D. Climate change and the vulnerability of electricity generation to water stress in the European Union. *Nat. Energy* https://doi.org/10.1038/nenergy.2017.114 (2017).
14. Grubert, E., Beach, F. & Webber, M. Can switching fuels save water? A life cycle quantification of freshwater consumption for Texas coal- and natural gas-fired electricity. *Environ. Res. Lett.* **7**, 045801 (2012).
15. Qin, Y. et al. Air quality–carbon–water synergies and trade-offs in China's natural gas industry. *Nat. Sustain.* **1**, 505–511 (2018).
16. Johst, M. & Rothstein, B. Reduction of cooling water consumption due to photovoltaic and wind electricity feed-in. *Renew. Sust. Energ. Rev.* **35**, 311–317 (2014).
17. Macknick, J., Sattler, S., Averyt, K., Clemmer, S. & Rogers, J. The water implications of generating electricity: water use across the United States based on different electricity pathways through 2050. *Environ. Res. Lett.* **7**, 045803 (2012).
18. Zhang, C., Anadon, L. D., Mo, H. P., Zhao, Z. N. & Liu, Z. Water–carbon trade-off in China's coal power industry. *Environ. Sci. Technol.* **48**, 11082–11089 (2014).
19. Macknick, J., Newmark, R., Heath, G. & Hallett, K. C. Operational water consumption and withdrawal factors for electricity generating technologies: a review of existing literature. *Environ. Res. Lett.* https://doi.org/10.1088/1748-9326/7/4/045802 (2012).
20. Jones, E., Qadir, M., van Vliet, M. T. H., Smakhtin, V. & Kang, S. M. The state of desalination and brine production: a global outlook. *Sci. Total Environ.* **657**, 1343–1356 (2019).
21. Jones, E. R., Vliet, M. T. H., Qadir, M. & Bierkens, M. F. P. Country-level and gridded estimates of wastewater production, collection, treatment and reuse. *Earth Syst. Sci. Data* **13**, 237–254 (2021).
22. Thorslund, J. & van Vliet, M. T. H. A global dataset of surface water and groundwater salinity measurements from 1980-2019. *Sci. Data* https://doi.org/10.1038/s41597-020-0562-z (2020).
23. van Vliet, M. T. H. et al. Global water scarcity including surface water quality and expansions of clean water technologies. *Environ. Res. Lett.* https://doi.org/10.1088/1748-9326/abbfc3 (2021).
24. Yu, X. Z. et al. Mapping research on carbon neutrality in WWTPs between 2001 and 2021: a scientometric and visualization analysis. *Sustain. Horizons* https://doi.org/10.1016/j.horiz.2022.100022 (2022).
25. Qin, Y. et al. Flexibility and intensity of global water use. *Nat. Sustain.* **2**, 515–523 (2019).
26. Ackerman, F. & Fisher, J. Is there a water–energy nexus in electricity generation? Long-term scenarios for the western United States. *Energ. Policy* **59**, 235–241 (2013).
27. Sovacool, B. K. & Sovacool, K. E. Preventing national electricity-water crisis areas in the United States. *Colum. J. Envtl. L.* **34**, 333 (2009).
28. Xing, X. et al. Spatially explicit analysis identifies significant potential for bioenergy with carbon capture and storage in China. *Nat. Commun.* **12**, 1–12 (2021).
29. Sanchez, D. L., Nelson, J. H., Johnston, J., Mileva, A. & Kammen, D. M. Biomass enables the transition to a carbon-negative power system across western North America. *Nat. Clim. Change* **5**, 230–234 (2015).
30. Wanders, N. & Wada, Y. Human and climate impacts on the 21st century hydrological drought. *J. Hydrol.* **526**, 208–220 (2014).
31. Wanders, N., Wada, Y. & Van Lanen, H. A. J. Global hydrological droughts in the 21st century under a changing hydrological regime. *Earth Syst. Dynam.* **6**, 1–15 (2015).
32. Qin, Y. Global competing water uses for food and energy. *Environ. Res. Lett.* **16**, 064091 (2021).
33. Vorosmarty, C. J., Green, P., Salisbury, J. & Lammers, R. B. Global water resources: vulnerability from climate change and population growth. *Science* **289**, 284–288 (2000).

34. Wei, Y. M. et al. A proposed global layout of carbon capture and storage in line with a 2 °C climate target. *Nat. Clim. Change* **11**, 112–118 (2021).

35. Irannezhad, M., Ahmadi, B., Liu, J., Chen, D. & Matthews, J. H. Global water security: a shining star in the dark sky of achieving the sustainable development goals. *Sustain. Horizons* https://doi.org/10.1016/j.horiz.2021.100005 (2022).

36. Tong, D. et al. Committed emissions from existing energy infrastructure jeopardize 1.5 °C climate target. *Nature* **572**, 373–377 (2019).

37. World Electric Power Plants (WEPP) Database 2017 Version (S&P Global Commodity Insights, 2018); https://www.platts.com/products/world-electric-power-plants-database.

38. Zhang, C., Zhong, L., Fu, X., Wang, J. & Wu, Z. Revealing water stress by the thermal power industry in China based on a high spatial resolution water withdrawal and consumption inventory. *Environ. Sci. Technol.* https://doi.org/10.1021/acs.est.5b05374 (2016).

39. Spang, E. S., Moomaw, W. R., Gallagher, K. S., Kirshen, P. H. & Marks, D. H. The water consumption of energy production: an international comparison. *Environ. Res. Lett.* **9**, 105002 (2014).

40. Delgado, A. & Herzog, H. J. A simple model to help understand water use at power plants. Massachusetts Institute of Technology Energy Initiative. Working paper. (2012).

41. Fricko, O. et al. Energy sector water use implications of a 2 °C climate policy. *Environ. Res. Lett.* **11**, 034011 (2016).

42. Sutanudjaja, E. H. et al. PCR-GLOBWB 2: a 5 arcmin global hydrological and water resources model. *Geosci. Model Dev.* **11**, 2429–2453 (2018).

43. Bosmans, J. et al. FutureStreams, a global dataset of future streamflow and water temperature. *Sci. Data* https://doi.org/10.1038/s41597-022-01410-6 (2022).

44. van Beek, L. P. H., Eikelboom, T., van Vliet, M. T. H. & Bierkens, M. F. P. A physically based model of global freshwater surface temperature. *Water Resour. Res.* **48**, W09530 (2012).

45. Wanders, N., van Vliet, M. T. H., Wada, Y., Bierkens, M. F. P. & van Beek, L. P. H. High-resolution global water temperature modeling. *Water Resour. Res.* **55**, 2760–2778 (2019).

46. *Technical Development Document for the Final Regulations Addressing Cooling Water Intake Structures for New Facilities. U.S. Environmental Protection Agency Office of Science and Technology Engineering and Analysis Division* (EPA, 2001).

47. Barbarossa, V. et al. Threats of global warming to the world's freshwater fishes. *Nat. Commun.* **12**, 1701 (2021).

48. Oki, T. & Kanae, S. Global hydrological cycles and world water resources. *Science* **313**, 1068–1072 (2006).

49. Baines, S., Wright, A., Lashko, E. & Robertson, H. *CO_2 Storage Resource Catalogue-Cycle 2. 10365GLOB-Rep-02-03* (Global CCS Institute, 2021).

50. Buscheck, T. A. et al. Combining brine extraction, desalination, and residual-brine reinjection with CO_2 storage in saline formations: implications for pressure management, capacity, and risk mitigation. *Energy Procedia* **4**, 4283–4290 (2011).

51. Gonzalez-Nicolas, A. et al. Pressure management via brine extraction in geological CO_2 storage: adaptive optimization strategies under poorly characterized reservoir conditions. *Int. J. Greenh. Gas Control* **83**, 176–185 (2019).

52. Breunig, H. M. et al. *Assessment of Brine Management for Geologic Carbon Sequestration* (Lawrence Berkeley National Laboratory, Environmental Energy Technologies Division, Indoor Environment Group, 2013).

53. Free vector and raster map data. *Natural Earth* https://www.naturalearthdata.com/ (2022).

Author contributions

Y.Q. and C.H. designed this study, Y.Q., Y.W., S.L., H.D., N.W., J.B., L.H. and C.H. analysed the data, Y.Q., E.B., D.G., J.M.B. and G.H. wrote the paper with input from all co-authors.

Competing interests

The authors declare no competing interests.

Additional information

Extended data is available for this paper at https://doi.org/10.1038/s44221-023-00120-6.

Supplementary information The online version contains supplementary material available at https://doi.org/10.1038/s44221-023-00120-6.

Correspondence and requests for materials should be addressed to Yue Qin or Chaopeng Hong.

Peer review information *Nature Water* thanks Vincent Tidwell, Kelly Sanders and the other, anonymous, reviewer(s) for their contribution to the peer review of this work.

**Reprints and permissions information** is available at www.nature.com/reprints.

Publisher's note Springer Nature remains neutral with regard to jurisdictional claims in published maps and institutional affiliations.

[1]The Key Laboratory of Water and Sediment Sciences, Ministry of Education, Peking University, Beijing, China. [2]College of Environmental Science and Engineering, Peking University, Beijing, China. [3]Institute of Carbon Neutrality, Peking University, Beijing, China. [4]Environmental Sciences Division and Climate Change Science Institute, Oak Ridge National Laboratory, Oak Ridge, TN, USA. [5]College of Engineering, Peking University, Beijing, China. [6]Department of Physical Geography, Utrecht University, Utrecht, The Netherlands. [7]Department of Environmental Science, Radboud University, Nijmegen, The Netherlands. [8]Shenzhen Key Laboratory of Ecological Remediation and Carbon Sequestration, Institute

of Environment and Ecology, Tsinghua Shenzhen International Graduate School, Tsinghua University, Shenzhen, China. [9]State Environmental Protection Key Laboratory of Sources and Control of Air Pollution Complex, Beijing, China. [10]International Institute for Applied Systems Analysis (IIASA), Laxenburg, Austria. [11]Department of Civil, Environmental, and Geodetic Engineering, The Ohio State University, Columbus, OH, USA. [12]Department of Integrated Systems Engineering, The Ohio State University, Columbus, OH, USA. [13]Sustainability Institute, The Ohio State University, Columbus, OH, USA. [14]John Glenn College of Public Affairs, The Ohio State University, Columbus, OH, USA. [15]Department of Technology and Society, Stony Brook University, Stony Brook, NY, USA. [16]Marxe School of Public and International Affairs, Baruch College, City University of New York, New York, NY, USA. ✉e-mail: qinyue@pku.edu.cn; hcp12@tsinghua.org.cn
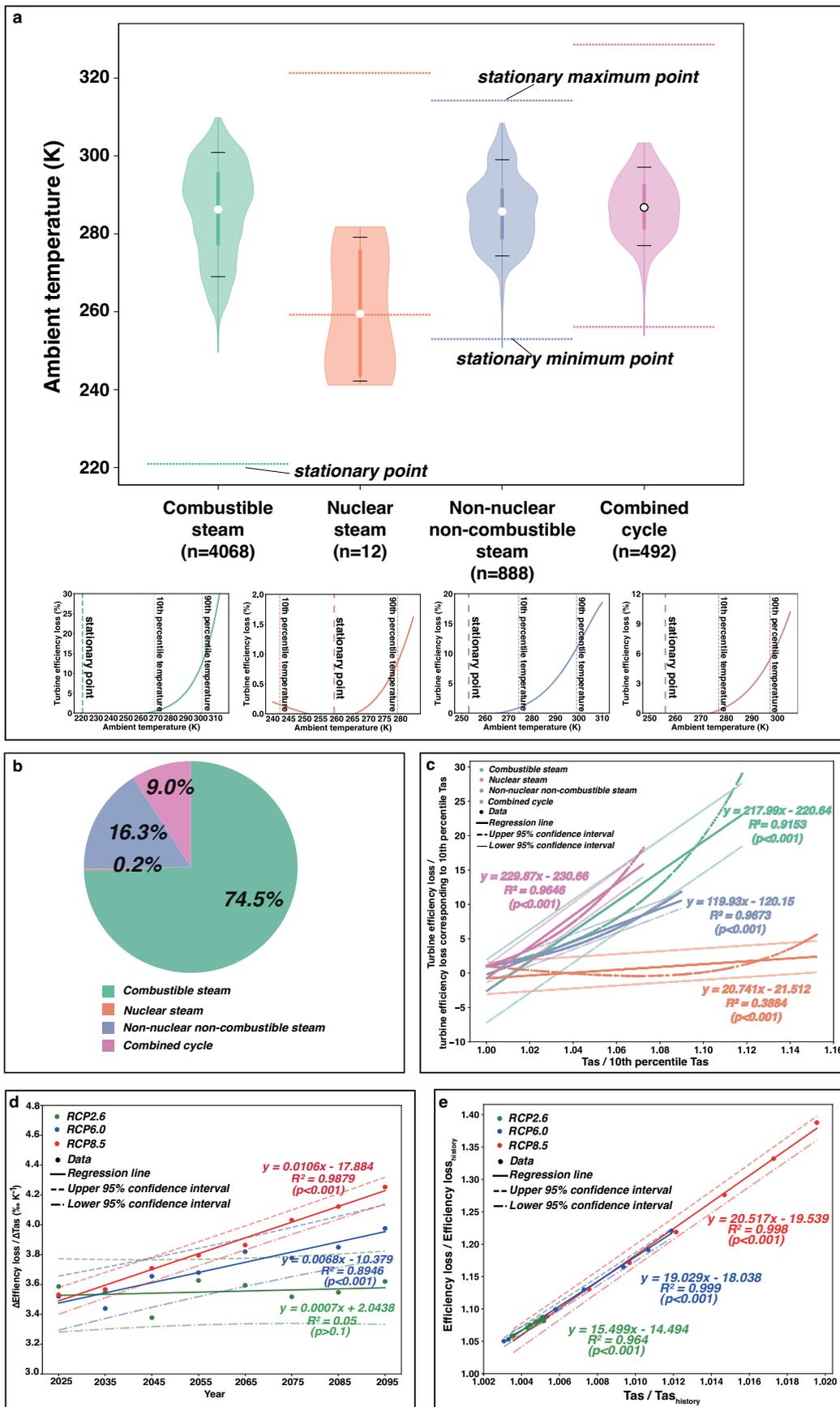
Extended Data Fig. 1 | See next page for caption.

Extended Data Fig. 1 | Unit-level and aggregated dry cooling units' efficiency loss against ambient temperature. (**a**) Exposure of unit-level dry cooling fleets with different engine types to monthly ambient temperature, and their corresponding turbine efficiency loss-temperature responses. n represents sample sizes. The mean (white dot), 25th and 75th percentiles (box), and 10th and 90th percentiles (botom and upper short black horizontal lines) are displayed, and minima/maxima are indicated by the violin plot range. The majority thermal units are exposed to ambient temperature either above its stationary point (for example, combustible steam) or between the minimum and maximum stationary points (as defined in Supplementary Table 1), thus are mostly demonstrating non-linear turbine efficiency loss increases with increasing temperature. (**b**) Relative share of different dry cooling engine types, which is dominated by combustible steam. (**c**) Relative increasing rates between unit-level turbine efficiency losses and ambient temperature (Tas), illustrating faster turbine efficiency loss increases than ambient temperature for different dry cooling engine types. (**d**) Slopes and corresponding linear regression for aggregated dry cooling fleets under different RCP scenarios in main text Fig. 4c, upper and lower 95% confidence interval indicate the 97.5th and 2.5th percentile, respectively. (**e**) Relative increasing rates between aggregated efficiency losses and corresponding ambient temperature (Tas).

nature portfolio

Corresponding author(s): Yue QIN and Chaopeng Hong

Last updated by author(s): Jul 11, 2023

Reporting Summary

Nature Portfolio wishes to improve the reproducibility of the work that we publish. This form provides structure for consistency and transparency in reporting. For further information on Nature Portfolio policies, see our Editorial Policies and the Editorial Policy Checklist.

Statistics

For all statistical analyses, confirm that the following items are present in the figure legend, table legend, main text, or Methods section.

n/a	Confirmed	
☐	☒	The exact sample size (*n*) for each experimental group/condition, given as a discrete number and unit of measurement
☒	☐	A statement on whether measurements were taken from distinct samples or whether the same sample was measured repeatedly
☒	☐	The statistical test(s) used AND whether they are one- or two-sided *Only common tests should be described solely by name; describe more complex techniques in the Methods section.*
☒	☐	A description of all covariates tested
☐	☒	A description of any assumptions or corrections, such as tests of normality and adjustment for multiple comparisons
☐	☒	A full description of the statistical parameters including central tendency (e.g. means) or other basic estimates (e.g. regression coefficient) AND variation (e.g. standard deviation) or associated estimates of uncertainty (e.g. confidence intervals)
☒	☐	For null hypothesis testing, the test statistic (e.g. *F*, *t*, *r*) with confidence intervals, effect sizes, degrees of freedom and *P* value noted *Give P values as exact values whenever suitable.*
☒	☐	For Bayesian analysis, information on the choice of priors and Markov chain Monte Carlo settings
☒	☐	For hierarchical and complex designs, identification of the appropriate level for tests and full reporting of outcomes
☒	☐	Estimates of effect sizes (e.g. Cohen's *d*, Pearson's *r*), indicating how they were calculated

Our web collection on statistics for biologists contains articles on many of the points above.

Software and code

Policy information about availability of computer code

Data collection	Water temperature and water discharge data are collected from PCRaster Global Water Balance model version 2 (PCR-GLOBWB 2) ; humidity, air temperature, pressure data are collected from ISIMIP project;
Data analysis	Python codes are used to process the data

For manuscripts utilizing custom algorithms or software that are central to the research but not yet described in published literature, software must be made available to editors and reviewers. We strongly encourage code deposition in a community repository (e.g. GitHub). See the Nature Portfolio guidelines for submitting code & software for further information.

Data

Policy information about availability of data

All manuscripts must include a data availability statement. This statement should provide the following information, where applicable:
- Accession codes, unique identifiers, or web links for publicly available datasets
- A description of any restrictions on data availability
- For clinical datasets or third party data, please ensure that the statement adheres to our policy

Water temperature and water discharge data are collected from PCRaster Global Water Balance model version 2 (PCR-GLOBWB 2) from the Inter-Sectoral Impact Model Inter-comparison (ISI-MIP) Project (https://www.isimip.org) ; Wastewater data are from Jones et al. (2021); Dry cooling generation units data are from the World Electric Power Plants (WEPP) database (2017 version); all other data are presented in the main text and Supplementary information.

Human research participants

Policy information about [studies involving human research participants and Sex and Gender in Research.](#)

Reporting on sex and gender	N/A
Population characteristics	N/A
Recruitment	N/A
Ethics oversight	N/A

Note that full information on the approval of the study protocol must also be provided in the manuscript.

Field-specific reporting

Please select the one below that is the best fit for your research. If you are not sure, read the appropriate sections before making your selection.

☐ Life sciences   ☐ Behavioural & social sciences   ☒ Ecological, evolutionary & environmental sciences

For a reference copy of the document with all sections, see [nature.com/documents/nr-reporting-summary-flat.pdf](#)

Ecological, evolutionary & environmental sciences study design

All studies must disclose on these points even when the disclosure is negative.

Study description	We analyze the water consumption (withdrawal) together with efficiency and CO2 emissions for unit-level dry cooling generation units; in addition, we integrate with alternative water sourcing and carbon storage information to explore solutions to address dry cooling associated carbon-water tradeoffs.
Research sample	Dry cooling generation units data are from the World Electric Power Plants (WEPP) database (2017 version)
Sampling strategy	We focus on dry cooling generation for primary fuel types (e.g., coal, gas, oil, biomass) that are potentially subject to efficiency loss and carbon-water traeoffs, generation units are from the World Electric Power Plants (WEPP) database (2017 version).
Data collection	Dry cooling generation units data are from the World Electric Power Plants (WEPP) database (2017 version), Water temperature and water discharge data are collected from PCRaster Global Water Balance model version 2 (PCR-GLOBWB 2) from the Inter-Sectoral Impact Model Inter-comparison (ISI-MIP) Project (https://www.isimip.org)
Timing and spatial scale	generation units data is collected for base year 2015; water temperature and water discharge data are collected for both the historical period (1996-2005) and till the end of century (e.g., 2020-2099).
Data exclusions	All thermal dry cooling units are included
Reproducibility	multiple climate models are used for reproducibility in obtaining water temperature and water discharge data are collected from PCRaster Global Water Balance model version 2 (PCR-GLOBWB 2) from the Inter-Sectoral Impact Model Inter-comparison (ISI-MIP) Project (https://www.isimip.org)
Randomization	we allocate dry cooling generation units by fuel types, geographic regions, and four seasons to evaluate
Blinding	Our analysis directly collects power generation units data and grid-level water temperature and water discharge data under different climate scenarios, which does not relate to blinding.

Did the study involve field work?   ☐ Yes   ☒ No

Reporting for specific materials, systems and methods

We require information from authors about some types of materials, experimental systems and methods used in many studies. Here, indicate whether each material, system or method listed is relevant to your study. If you are not sure if a list item applies to your research, read the appropriate section before selecting a response.

Materials & experimental systems

n/a	Involved in the study
☒	Antibodies
☒	Eukaryotic cell lines
☒	Palaeontology and archaeology
☒	Animals and other organisms
☒	Clinical data
☒	Dual use research of concern

Methods

n/a	Involved in the study
☒	ChIP-seq
☒	Flow cytometry
☒	MRI-based neuroimaging